Reactions of Metal Cluster Ions**

Pierre Fayet*

In order to prove their extraordinary behaviour as a function of size, metal cluster ions, generated by sputtering, were investigated by a variety of experiments. In the gas phase, synthesis of size-selected nickel carbonyl clusters was carried out in a triple quadrupole mass spectrometer. The cluster compounds showed a sensitive photodetachment of ligands, which allows the full control of their CO coverage with laser desorption. The deposition of silver clusters on photographic films has revealed their catalytic activity during the development process, providing fascinating future perspectives.

Pierre Fayet: Born 1954 in Montreux. Received his Ph. D. in physics 1987 from the Ecole Polytechnique Fédérale de Lausanne (EPFL), where he worked at the Institut de Physique Expérimentale in the research group of Dr. Ludger Wöste. He joined Exxon Research and Engineering Company, Annandale, New Jersey, in October 1987, in order to perform catalytic experiments on size-selected clusters, as outlined in the last chapter of this article.

1. Introduction

Metal clusters are commonly associated with the very fundamental role of bridging the gap from atoms and small molecules to the bulk [1]. Moreover, they have extraordinary chemical properties, which are due to their structure and electronic behaviour. Over more than two decades spectroscopic information on matrix-isolated particles has provided some conceptions of catalytic processes occurring on metal surfaces [2]. There are, however, obvious attractions of working in the gas phase, since one can avoid complications arising from matrix effects.

Molecular beam techniques combined with mass spectrometry have proved to be very powerful tools for investigating physical and chemical properties of metal clusters of a specific size. This is documented by a series of impressive results, which – combined with new computational methods – contributed to the evolution of cluster science from what was originally a purely empirical field to a discipline where quantum mechanical understanding is verified by well-designed experiments. The development of the electronic shell model by *Knight* et al. [3] provided an conspicuous example. A bridge between spectroscopic properties of metal clusters and their corresponding chemical properties was established by *Whetten* et al. [4] who measured and correlated the ionization potentials of iron clusters and the corresponding hydrogen absorption affinities as a function of their size. The results prove that the investigation of spectroscopic and chemical properties of metal clusters contributes to the understanding of such particles, as well as indicating a way to future applications.

2. Production of Size-Selected Metal Clusters

Since cluster beam sources usually generate size distributions, experiments on size-selected clusters require the use of mass spectrometry. This suggests sources that directly produce ionized clusters.

High currents of cluster ions are conveniently generated in the sputtering process by bombarding a target with fast atom or ion beams. In order to produce large cluster currents, the extraction ion optics of the cluster transport line must be close to the target. This constraint places the primary ion source quite far away from the target. Thus the source must be of low divergence, but must provide a large current. This requirement is fulfilled by the extreme brightness of the cold reflex discharge ion source (CORDIS) developed by *Keller* [5].

Fig. 1 shows a sectional view of CORDIS. The primary electrons are generated by six resistively heated tantalum filaments suspended on a molybdenum rod near the source axis. 18 permanent magnets placed around the anode restrict the plasma electrons into the loss zones only. These zones are the magnetic field lines of the cusps across the anode wall. This configuration creates a cylindrical plasma of uniform density over a diameter of 3.5 cm. The source is operated with argon at 4 Pa of pressure as measured near the gas inlet tube. $Ar^{\oplus}$ ions are extracted by the accel/decel lens system at 20 keV. The negatively biased intermediate electrode focuses secondary electrons created in the extraction zone by the ionizaton of the argon residual gas. Since the positive space charge of the $Ar^{\oplus}$ ion beam is balanced by the presence of electrons, ions are strongly focused over a long distance. A beam current up to 10 mA can thus be measured on the target, even if it is positioned 50 cm away from the source outlet plane.

When combined with a quadrupole mass spectrometer, the sputtering arrange-

* *Correspondence:* Dr. P. Fayet
Exxon Research and Engineering Company
Clinton Township, Route 22 East
Annandale, NJ 08801 (USA)

** This article is based on a lecture presented at the «6ème Journée d'Analyse GACHI: L'analyse de composés non-volatils par spectrométrie de masse» in Lausanne, October 15, 1987. The work described therein, has been performed at the Institut de Physique Expérimentale, EPFL.

ment is a powerful source of size-selected cluster ions. Indeed, quadrupole mass spectrometers have extremely high transmission functions under decent resolution values. This allowed us to obtain particle beams of $Ag_3^{\oplus}$ up to 10^{12} particles per second[6]. A further advantage of quadrupole mass spectrometers is the low ion energy (< 20 eV) needed to filter and guide ions. This feature allows ion-molecule reactions at low energy and the deposition of filtered particles in the «soft-landing mode» without the necessity of slowing down the ion beam (cf. Section 6).

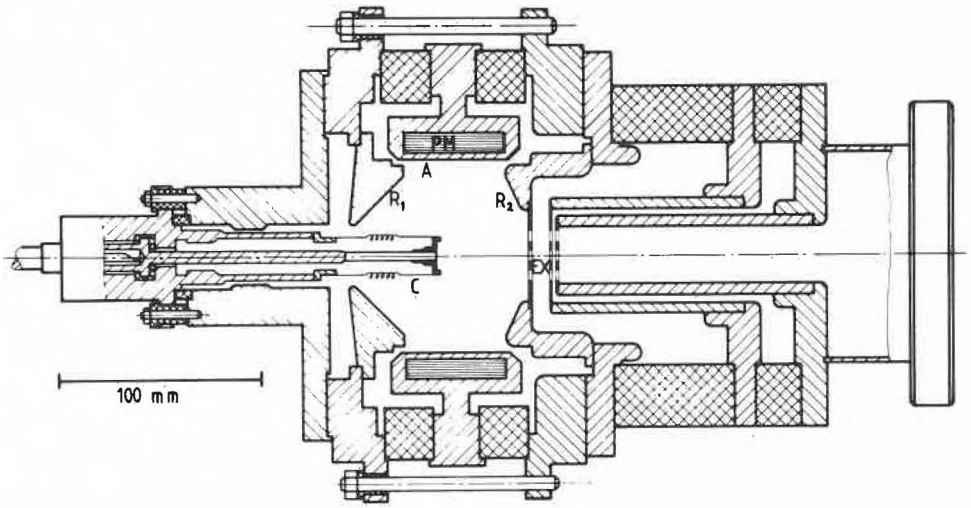

Fig. 1. Sectional view of the sputter ion source CORDIS, developed by Keller[5]*. Using argon, the source enables one to obtain at 20 kV extraction voltage typical primary ion currents on the target (diameter 8 mm) of 2 mA. – A: anode; C: cathode; EX: extraction plates, here: accel/decel-system; PM: permanent magnets; R_1: reflector electrode on cathode side; R_2: reflector on extraction side, bearing the outlet electrode.*

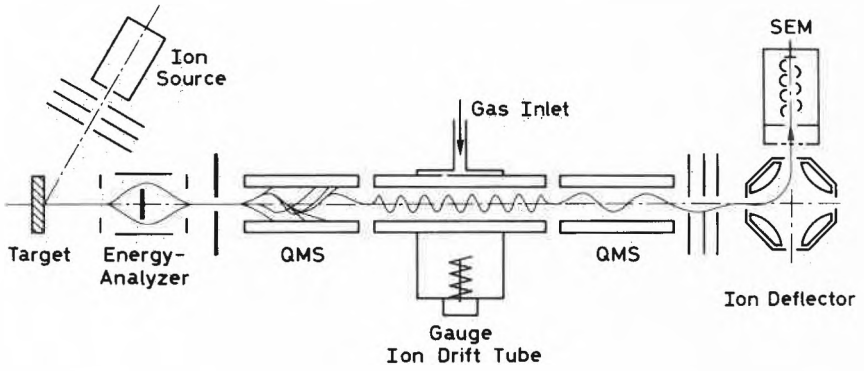

Fig. 2. Triple quadrupole arrangement for performing experiments on size-selected metal clusters: The particles are produced by sputtering, energy-analyzed, mass-filtered, and introduced into the ion drift tube. All inelastic scattering events are recorded with a subsequent quadrupole mass analyzer.

3. Experimental Set-Up

The experimental scheme is shown in Fig. 2: The cluster ions are produced, as explained in Section 2, by means of sputtering. The kinetic energy distribution of sputtered particles in typically between 0 and 10 eV. A cylindrical retarding field energy analyzer allows the selection of an increment of 2 eV. In addition, it blocks all fast primary ions and sputtered neutrals. The energy filter is directly mounted at the entrance of the quadrupole mass filter at a distance of about 4 cm from the target. We used a commercial quadrupole rod system of 9.5 mm pole diameter and a length of 20 cm (Extranuclear Model 4-162-8), which reaches under normal operating conditions a maximum mass value of 1700. In a modified version we were able, however, to reach mass values up to 9500[7]. The monodispersed cluster beam is directly guided from the quadrupole mass filter into a RF ion drift tube, which is 60 cm long and has an identical sectional view to the mass filter. The drift tube is operated with the same RF frequency as the mass filter at a controlled phase shift. Since no dc voltage is applied, there is no mass discrimination, and all ions, reaction products or photofragments, are kept in confinement. The bias potential of the rod system allows the confined ions to be slowed down to almost thermal velocities, which correponds to residence times of up to $\approx$ 10 ms. The drift tube is surrounded by a scatter chamber of 10 cm length, where reactant gas can be introduced. The complete drift tube assembly is placed inside another differentially pumped ultra-high vacuum chamber, pumped by a 500 L/s turbomolecular pump. The background pressure under normal operation conditions is 10^{-8} mbar, which is sufficient to prevent undesired background collisions. It can be operated, however, at a pressure up to 10^{-2} mbar, when reactant gas is introduced. At the exit of the drift tube the confined ion beam enters another quadrupole mass filter (Extranuclear Model 4-162-8), which is operated at the same frequency as the first mass filter at a controlled phase shift. It is placed inside a differentially pumped ultra-high vacuum chamber pumped by a 500 L/s turbomolecular pump. The same chamber also contains a 21-stage Cu-Be secondary electron multiplier for detecting the ions. It is mounted on an electrostatic ion deflector, allowing a laser beam to enter the triple quadrupole system in order to interact with the confined particles.

Fig. 3a shows the mass spectrum of sputtered $Ni_n^{\oplus}$ clusters that was obtained when the final quadrupole mass filter is scanned, while the first quadrupole mass filter is kept – like the drift tube – in an ion-confinement mode at RF only. When the first quadrupole mass filter is set – by adding a dc voltage – into a discriminative mode, only clusters of a well-defined size can enter the drift tube. So the final quadrupole mass filter detects the signal of a monodispersed cluster beam (see Fig. 3b, where the first quadrupole was set to the mass of $Ni_4^{\oplus}$). The introduction of a reactant gas into the ion drift tube enables one to perform and trace ion-molecule reactions with cluster ions of any desired size and energy.

4. Cluster-Molecule Reactions

If one simultaneously introduces size-selected cluster ions and carbon monoxide into the drift tube, carbonylnickel ions $[Ni_n(CO)_k]^{\oplus}$ and carbidocarbonylnickel ions $[Ni_nC(CO)_l]^{\oplus}$ are revealed by scanning the last quadrupole. An example is shown in Fig. 4a for a beam of $Ni_4^{\oplus}$ with a kinetic energy of 2 eV and a CO pressure in the ion drift tube of 2.0×10^{-4} mbar. $Ni_4^{\oplus}$ mother ions react with one or several CO molecules before leaving the interaction zone. The ligand distribution, which exhibits an exponentially decreasing pattern, indicates that the reaction is not yet completed. More CO molecules can be added to the metal core. The CO pressure is then gradually increased to the point at which the mass spectrum no longer changes; i.e., when saturation of clusters by carbon monoxide ligands occurs (CO pressure: 2.4×10^{-3} mbar). This situation is depicted in Fig. 4b. The mass spectrum

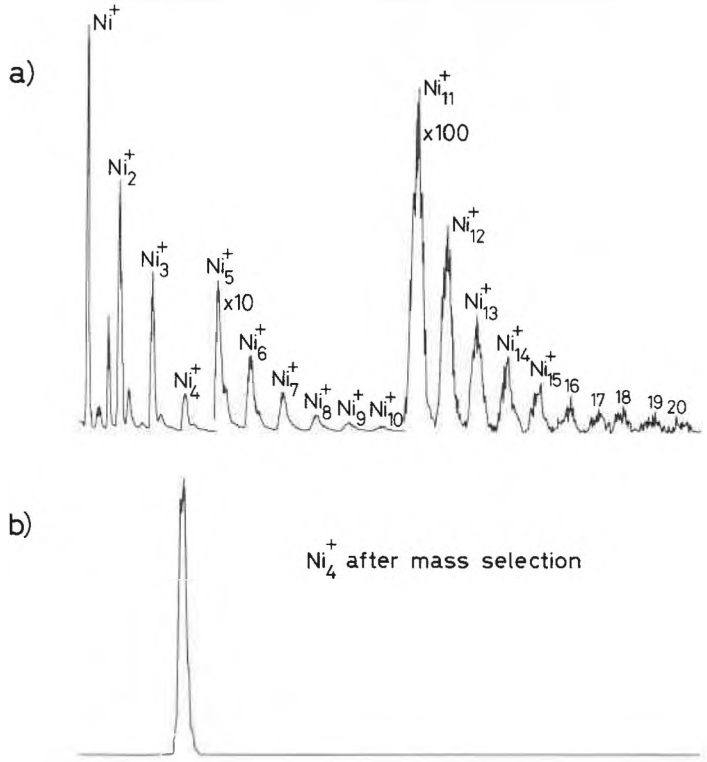

Fig. 3. a) Mass spectrum of sputtered nickel aggregates obtained by setting the first QMS and drift tube on RF only, while the last QMS was scanned. – b) Mass spectrum of a monodispersed cluster beam obtained by setting the first QMS on the mass of $Ni_4^{\oplus}$ while the last QMS was scanned.

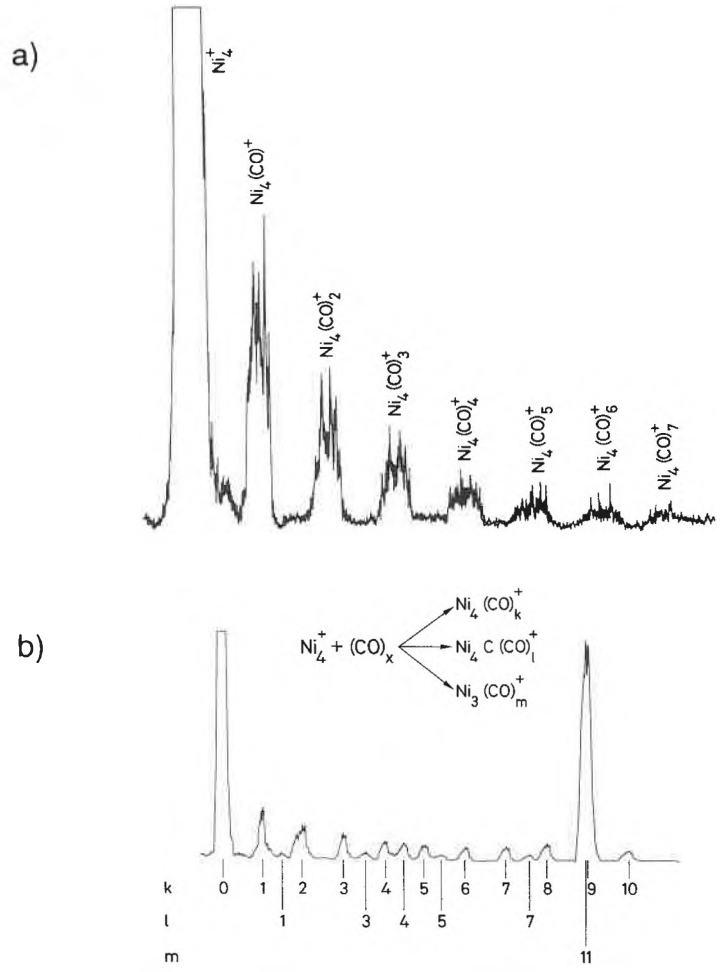

Fig. 4. Reactive clustering of CO ligands to a $Ni_4^{\oplus}$ cluster on introducing carbon monoxide into the drift tube: (a) at a CO pressure of 3×10^{-4} bar, the synthesis of saturated compounds is not yet achieved; (b) at a CO pressure of 3×10^{-3} bar, the system $[Ni_4(CO)_{10}]^{\oplus}$ appears clearly as the saturated compound.

clearly shows that no further carbonyl complexes are observed after $[Ni_4(CO)_{10}]^{\oplus}$. This indicates that $Ni_4^{\oplus}$ compounds are saturated with 10 CO ligands. The strong resonance on the mass of $[Ni_4(CO)_9]^{\oplus}$ is due to the charge of the incident tetramers. The missing electron diminishes the cluster capability to become saturated. Applying the simple 18-electrons rule («electron counting») to this situation, the fully occupied s-, p-, and d-orbitals accommodate $4 \times 8 = 72$ electrons. The four nickel atoms provide 40 electrons, the ten carbonyl ligands contribute another 20 electrons. This leaves 12 electrons to establish the metal skeleton. This represents six metal-metal bonds in the most compact structure of a tetrahedron, having four terminal and six bridging carbonyl ligands (Fig. 5).

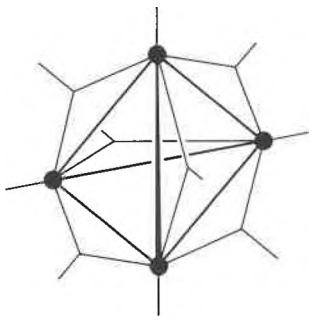

Fig. 5. Structure of $[Ni_4(CO)_{10}]$ exhibiting four terminal and six bridging CO ligands.

The stoichiometry of larger aggregates shows fairly large deviations from the 18-electrons rule, due to a large promotion energy between the s- and p-orbitals found for the free atom[15]. Thus, the bonding capacity of a given metal will depend upon the relative energy of the p-orbitals. Simple electron-counting rules exist to correlate molecular geometries of metal cluster compounds with the total number of valence electrons. Since individual CO ligands rapidly exchange positions over the metal core, there is no one arrangement that is energetically preferred over all others[8,9]. Indeed, it is apparent that individual ligands interact with the cluster as a whole and not just with individual atoms.

The close analogies between this situation and the bonding of the so-called electron deficient boranes, B_nH_m, have been recognized by *Wade*[10] and *Mingos*[11]. They established empirical rules[12,13] based on the same delocalized molecular orbitals. These ideas have also been extended to account for some aspects of the reactivity of organometallic clusters[14]. Of particular relevance to our results is the work of *Lauher*[15] who not only calculated the most favourable molecular geometry for any given transition-metal cluster but also predicted the bonding capabilities of such clusters. The original calculations were

based on clusters of rhodium atoms, but the results are readily transferable to most other transition metals. Since that time, many of *Lauher*'s predictions have been experimentally verified[16]. The application of this rule to nickel carbonyls leads to the «core» structures shown in Fig. 6[17]. The corresponding number of ligands is given in Table 1. The predicted values are surprisingly close to the results we have observed experimentally. The observation verifies the validity of *Lauher*'s predictions. It shows furthermore that stoichiometrically reasonable results can be obtained with size-selected metal clusters in the proposed triple quadrupole arrangement (Fig. 2).

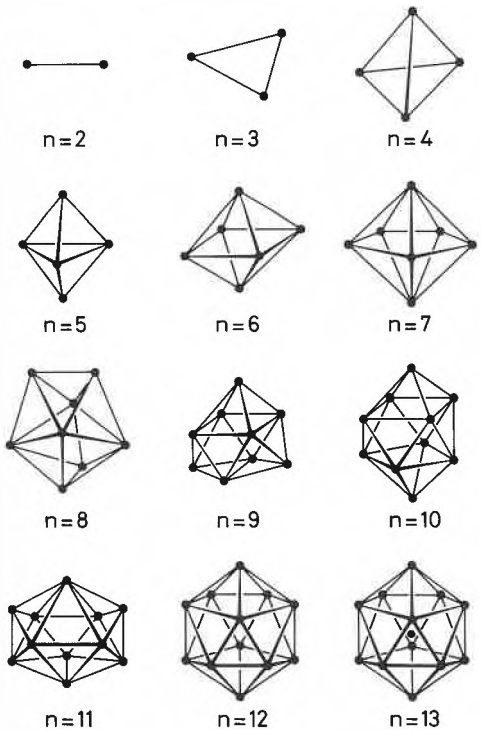

Fig. 6. Shapes of the metallic skeleton of the saturated cluster compounds $[Ni_n(CO)_m]$ as predicted and measured according to Table 1[16].

5. Photochemistry

The saturation experiments of the cluster surface help us to understand the bonding capability of metal clusters and their geometrical structure. They are, however, unable to explain either the kinetics of reactions or the energetics of chemical bonds. Further insight into the bonding between clusters and adsorbed molecules can be obtained by a change of the equilibrium conditions of the reaction. As the CO coverage of nickel clusters can be different for different initial reactant pressures (Fig. 4), an excitation of the metallic core also changes the distribution of final products. For this purpose nickel carbonyls were irradiated with an $Ar^{\oplus}$-laser beam positioned along the ion drift tube axis (see Fig. 2). An example for the ligand system of $[Ni_{10}(CO)_x]^{\oplus}$ is shown in Fig. 7.

Table 1. Predicted and observed CO bonding capabilities of $Ni_n^{\oplus}$ clusters.

Cluster	$Ni_2^{\oplus}$	$Ni_3^{\oplus}$	$Ni_4^{\oplus}$	$Ni_5^{\oplus}$	$Ni_6^{\oplus}$	$Ni_7^{\oplus}$	$Ni_8^{\oplus}$	$Ni_9^{\oplus}$	$Ni_{10}^{\oplus}$	$Ni_{11}^{\oplus}$	$Ni_{12}^{\oplus}$	$Ni_{13}^{\oplus}$
maximum quantity of predicted CO ligands	7	9	10	11	13	15	17	19	21	23	25	20
maximum quantity of observed CO ligands	9	8	10	12	13	15	16	17	18	19	20	20*)

*) Very small peak appearing for 21 and 22.

With no laser irradiation the system accumulates CO ligands until $[Ni_{10}(CO)_{18}]^{\oplus}$ is formed. The strongest peak occurs at $[Ni_{10}(CO)_{17}]^{\oplus}$, which is due to the missing electron. When 10 mW laser power of the 488 nm line of an argon laser was applied, the mass peaks of the saturated complexes began to lose intensity. The phenomenon gradually increased at 30 mW; and at 100 mW no signal appeared for $[Ni_{10}(CO)_{17}]^{\oplus}$ and $[Ni_{10}(CO)_{18}]^{\oplus}$. Further ligands were stripped at 300 mW, and at a laser power of 900 mW no more ligands were seen and even the mother ion $Ni_{10}^{\oplus}$ exhibited an increased fragmentation tendency towards $Ni_9^{\oplus}$, $Ni_8^{\oplus}$, and $Ni_7^{\oplus}$.

The result shows that efficient photochemical reaction channels are present. The efficiency of this process increased when the wavelength was shortened[18]. Since the CO molecules are transparent to the range of used wavelengths (lines of the $Ar^{\oplus}$-laser), CO desorption was due to a transfer of the metallic core electronic excitation to the metal-carbon bond. The photoabsorption cross section is of the order of 1.4×10^{-18} cm^2 for $Ni_4^{\oplus}$; it appears to increase with growing cluster size. This change of magnitude, together with the wavelength dependence, indicated collective electronic excitations of the metal cluster.

During the experiment the ion drift tube served two purposes: 1) the synthesis of the metal carbonyls, 2) the photodesorption of the attached CO ligands. It is obvious that more sophisticated instruments like quintuple quadrupole or ICR traps would allow to observe both phenomena separately.

6. Deposition of Ionized Clusters – Future Perspectives

A system such as metal-carbonyl complexes is of great interest for applications in catalysis. The large electronic excitation cross section of the metallic core also raises

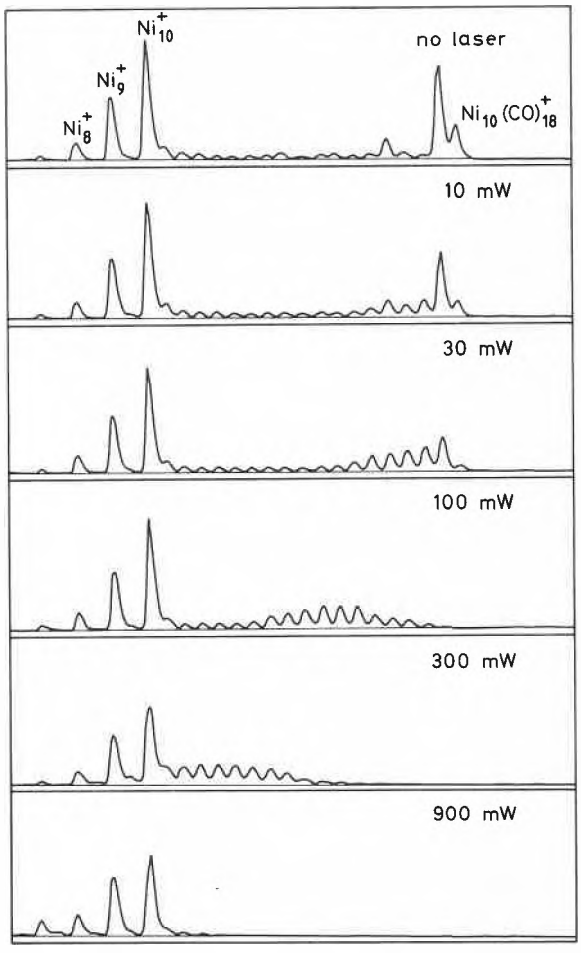

Fig. 7. Progressive stripping of CO ligands from $[Ni_{10}(CO)_{18}]^{\oplus}$ by means of photoexcitation of the metallic core ($\lambda = 488$ nm) [17].

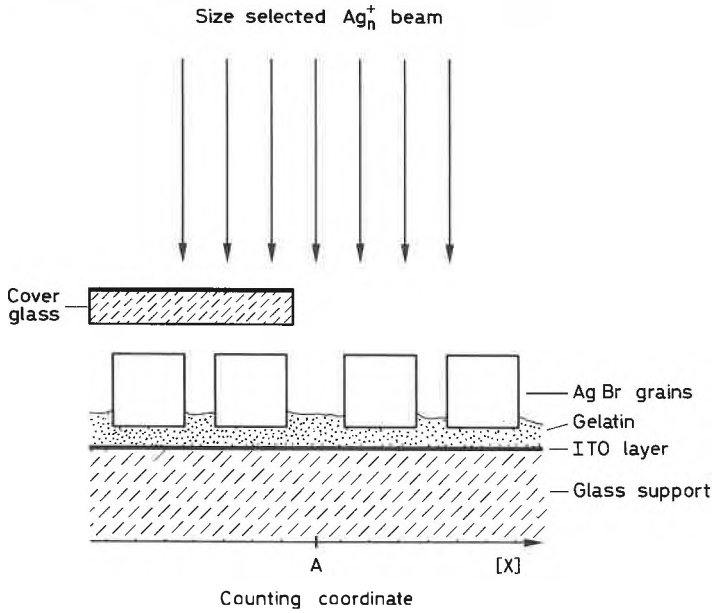

Fig. 8. Experimental scheme for depositing monodisperse silver cluster ions on a photographic plate. The ITO (indium tin oxide) layer prevents the build-up of repulsive charge.

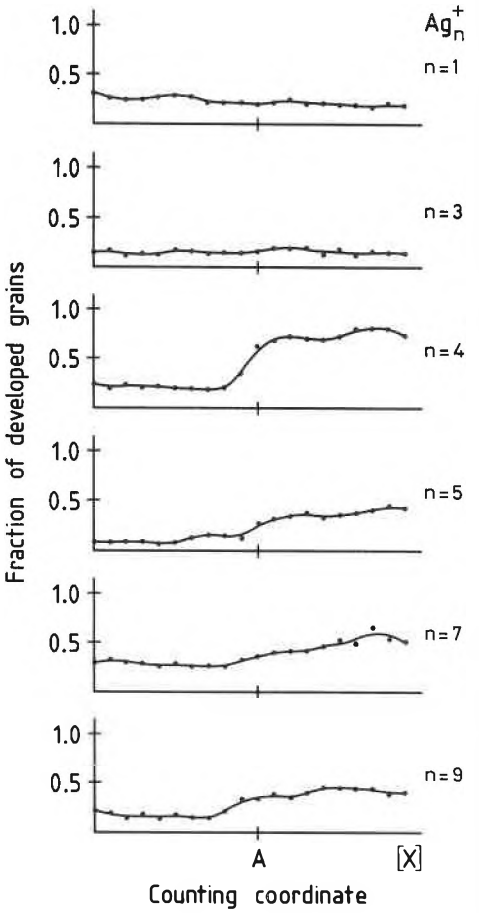

Fig. 9. Fraction of developed grains vs. counting coordinate X. The result proves, that $Ag_n^\oplus$ clusters ($n \geq 4$) deposited on a photographic plate create latent image specks [19].

the possibility for photon-induced catalysis. Experiments in the gas phase are sensitivity limited, because the number of three-body collisions in the above mentioned experimental scheme (Fig. 2) is low. This suggests depositing the size-selected particles on a surface.

A classical system where metal clusters most likely have extraordinary catalytic properties is the silver photographic system. Photographic plates consist of silver halide microcrystals (sized between 0.1 to several μm) supported on a substrate. All models, which describe elementary processes between the light and the silver halide, conclude that with light exposure, formation of a latent image speck occurs on the silver halide crystal. The immersion of the plate in the development bath creates the real image by reduction of crystals containing specks to metallic silver. The process is considerably slower for unexposed crystals, containing no specks. There is a fair agreement, that the latent image speck is not atomic silver, but it should be a cluster[19].

We exposed, therefore, photographic plates to beams of size-selected silver cluster ions $Ag_n^\oplus$ (n = 1–9)[20]. The photographic specimens consisted of binder-free AgBr monocrystals sedimented onto a gelatin-coated glass plate (see Fig. 8). The grain shape was cubic with a length of 0.8 μm. In addition, the glass plate was coated with a thin conductive layer of indium tin oxide to prevent charging up during deposition. The radiation dose was chosen such that approximately 10 clusters were deposited on each AgBr grain. Half of the irradiated area was covered with a conductive glass plate to compensate for a spurious light background which could come from the primary ion source. The irradiated plates were then taken out of the vacuum and developed by using a conventional developer.

The results we obtained for irradiation with different cluster sizes are shown in Fig. 9: The deposited clusters cause no change on the photographic plate for cluster sizes between $Ag^\oplus$ and $Ag_3^\oplus$. At $Ag_4^\oplus$, however, more than 90% of the irradiated crystals became developable within the cluster-treated area. An increased developability of about 40% is also observed at larger cluster sizes. This may be due to fragmentation phenomena during the deposition process, or due to a threshold behaviour of the process, which at this point cannot be conclusively decided[20].

The experiment shows, however, that clusters of individual size do exhibit extraordinary catalytic properties, and that they can be successfully deposited on surfaces, even if some impact fragmentation occurs while they are deposited.

The outcome of the experiment encourages us to propose the following experimental scheme (see Fig. 10): Metal clusters are generated by means of sputtering, energy-filtered, mass-filtered, and deposited on an inert target at the lowest possible

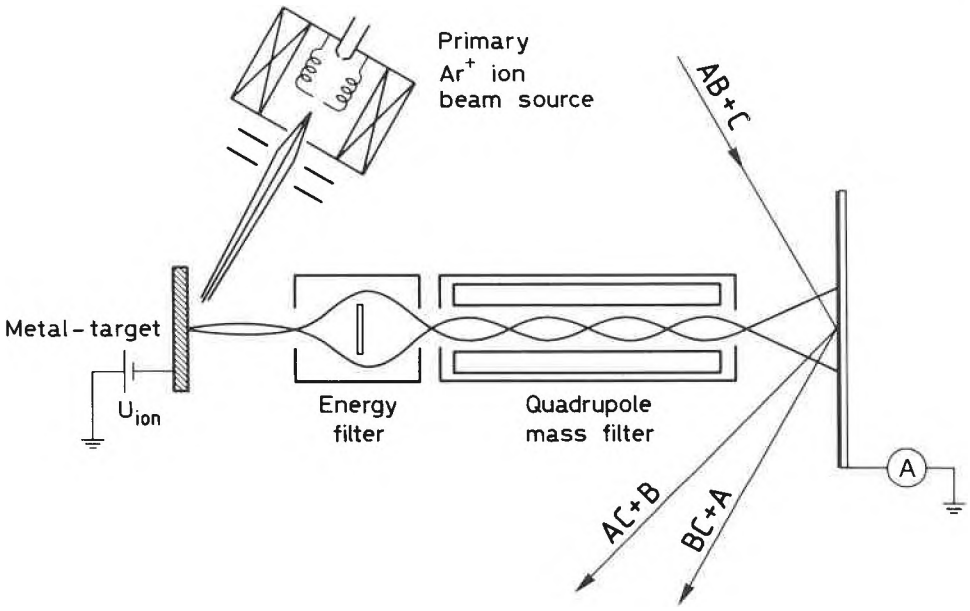

Fig. 10. Experimental set-up proposed for studying the catalytic properties of metal clusters of a specific size.

energy ($E_{kin} < 2$ eV). Simultaneously, the molecular beam of a catalytic reaction system is scattered on the target. Resulting catalytic reactions are observed by a mass-spectrometric analysis of the scattered particle beam. Hopefully my research stage at Exxon will prove the validity of this idea!

Acknowledgements: The experiments described in this account are the result of a very close and fruitful collaboration with my thesis adviser, Ludger Wöste. In addition to that we enjoyed very stimulating collaborations with other research groups, and I would like to express my gratitude to several colleagues: Roderich Keller provided the CORDIS design; Michael McGlinchey established the organometallic understanding for the carbonyl systems; Catherine and Philippe Bréchignac and Winston Saunders participated in the ligand-stripping experiment; Erik Moisar, Bernard Pischel, Gerd Hegenbart, and Friedrich Granzer performed together with us the photographic experiment.

Received: June 27, 1988 [FR 61]

[1] E. Schumacher, F. Blatter, M. Frey, U. Heiz, U. Röthlisberger, M. Schär, A. Vayloyan, C. Yeretzian, *Chimia 42* (1988) 357.
[2] M. Moskovits, G.A. Ozin (Ed.): *Cryochemistry*, Wiley-Interscience, New York (1979).
[3] W.D. Knight, K. Clemenger, W.A. de Heer, W.A. Saunders, M.Y. Chou, M.L. Cohen, *Phys. Rev. Lett. 52* (1984) 2141.
[4] R.L. Whetten, D.M. Cox, D.J. Trevor, A. Kaldor, *Phys. Rev. Lett. 54* (1985) 1494.
[5] R. Keller, *Proc. Workshop on High-Current, High-Brightness, and High Duty-Factor Ion Injectors*, San Diego CA (1985).
[6] P. Fayet, L. Wöste, *Z. Phys. D3* (1986) 177.
[7] P. Fayet, J.P. Wolf, L. Wöste, *Phys. Rev. B33* (1986) 6792; see also G. Delacrétac, P. Fayet, J.P. Wolf, L. Wöste, «Optical and dynamic properties of metal clusters», in G. Benedek, T.P. Martin, G. Paccioni (Ed.): *Elemental and Molecular Clusters*, Springer Ser. Mater. Sci., Vol. 6, p. 64–95, Springer, Berlin (1988).
[8] F.A. Cotton, J.D. Jamerson, *J. Am. Chem. Soc. 98* (1976) 1273.
[9] R.E. Benfield, B.F.G. Johnson, *J. Chem. Soc. Dalton Trans.* (1980) 1743.
[10] K. Wade, *Adv. Inorg. Chem. Radiochem. 18* (1976) 1.
[11] D.M.P. Mingos, *J. Chem. Soc. Dalton Trans.* (1974) 133.
[12] D.M.P. Mingos, *Acc. Chem. Res. 17* (1984) 311.
[13] D.M.P. Mingos, *Chem. Soc. Rev. 15* (1986) 31.
[14] M.J. McGlinchey, M. Mlekuz, P. Bougeard, B.G. Sayer, A. Marinetti, J.Y. Saillard, G. Jaouen, *Can. J. Chem. 61* (1983) 1319.
[15] J.W. Lauher, *J. Am. Chem. Soc. 100* (1978) 5305.
[16] B.F.G. Johnson, in B.F.G. Johnson (Ed.): *Transition Metal Clusters*, Wiley-Interscience, New York (1980).
[17] P. Fayet, M.J. McGlinchey, L. Wöste, *J. Am. Chem. Soc. 109* (1987) 1733.
[18] C. Bréchignac, P. Bréchignac, P. Fayet, W.A. Saunders, L. Wöste, *J. Chem. Phys. 89* (1988) 2419.
[19] T.H. James: *The Theory of Photographic Process, 4th Ed.*, Macmillan New York (1977).
[20] P. Fayet, F. Granzer, G. Hegenbart, E. Moisar, B. Pischel, L. Wöste, *Phys. Rev. Lett. 55* (1985) 3002.